

Structure-based Virtual Screening, and Design of Some Lead Compounds as Inhibitors of Kras-G12D of Pancreatic Cancer

Idris Momohjimoh Ovaku^{1*}, Stephen Eyije Abechi¹, Gideon Adamu Shallangwa², Abdullahi Bello Umar², Adamu Uzairu²

¹Department of Chemistry, Federal University of Lafia, P.M.B 146, Nasarawa State, Nigeria ²Department of Chemistry, Ahmadu Bello University, P.M.B 1044, Zaria, Kaduna State Nigeria

Abstract

Pancreatic cancer is an abnormal cell growth in the pancreas. In 2021, approximately 60,430 individuals were diagnosed in the USA, with the annual increasing incidence rates. Pancreatic cancer is anticipated to become the second leading cause of cancer mortality by 2030. This escalating challenge has prompted a search for innovative therapeutic agents. Virtual screening, a computational technique, was employed to discover novel drug-like compounds from a diverse set of 30 chemical compounds, sourced from the PubChem database. These compounds were evaluated based on some important properties, including pharmacokinetics, lipophilicity, drug-likeness, water-solubility, and physicochemical characteristics. Seventeen compounds emerged as promising candidates for pancreatic cancer treatment. Subsequent molecular docking studies focused on the Kras-G12D protein target and identified Ligand 18 as the leading candidate, exhibiting a binding energy (BE) of -10.5 kcal mol-1 and extensive interactions with the target protein. Additionally, a newly designed compound, D4, displayed an even higher BE of -10.8 kcal mol-1, fitting more effectively into the protein's binding site than existing drugs like Gemcitabine and Irinotecan. All newly designed compounds met the five scientists' rule, indicating favorable drug-likeness and bioavailability. These findings pave the way for developing a new generation of less toxic therapeutic compounds for pancreatic cancer treatment.

Keywords: virtual screening, binding energy, kras-G12D, pancreatic cancer, designed compounds.

INTRODUCTION

Cancer is the abnormal growth of the cells, and the part of the cell that grows abnormally is named after the cancer (Gupta, *et al.*, 2021). Pancreatic cancer is the irregular increase in the size of certain cells of the pancreas and it is ranked as the number four most common cause of cancer death in both men and women (Carioli, *et al.*, 2021). It affects

mostly aged people, with an average diagnostic age of 71 years for men and 75 years for women (Ducreux, *et al.*, 2015). The highest incidences of pancreatic cancer are reported in Europe and North

Submitted: November 12, 2024

Revised: December

Accepted: December 19, 2024 Published online: January 21, 2025

*Corresponding author: eedrismj@gmail.com



America and the lowest incidences are in Eastern Africa and South-Central Asia (Bray, et al., 2018). Kras mutation known as G12D is the most common mutation in pancreatic cancer and it is present in about 35% of people diagnosed with the disease (Dai, et al., 2022). The KRAS protein usually turns on and off like a switch. In response to certain signals, it becomes activated and then encourages the cell to grow and divide. When the signals are no longer present, it turns off. However, some mutant forms of KRAS (G12D), remain active even in the absence of growth signals, leading to uncontrolled cell growth (Dai, et al., 2022). All efforts made to develop drugs that block the cancer-fuelling effects of mutant KRAS proteins have been unsuccessful. Recently, a new drug, known as MRTX1133 was found to have a promising result in the models of Pancreatic cancer, and it is the first KRAS-blocking drug and targeted therapy of any kind (Hofmann, et al., 2022). Other drugs such as Gemcitabine, Fluorouracil, Irinotecan, and so on, were also found to be effective in treating the disease. Despite this recent progress, researchers are still in search of a way to develop a more prominent drug candidacy with fewer side effects. This work therefore aims to

design lead compounds with better efficacy for the treatment of pancreatic cancer.

Virtual screening is a computational approach employed to evaluate virtual libraries of databases, as *in silico* laboratories, against virtual receptors (targets) to speed up the drug discovery process (Patel, *et al.*, 2021). It is built for searching large hypothetical databases of chemical structures or virtual libraries for selecting a few numbers of candidate molecules that may be active against a chosen biological receptor (da Silva Rocha, *et al.*, 2019). Several promising compounds can be identified through virtual screening and subsequently validated in laboratory experiments.

Molecular docking is one of the two main approaches to the virtual screening of large databases of chemical compounds (Banegas-Luna, *et al.*, 2018). It is used to predict the binding geometry of compounds within the binding site of the target protein model (Broomhead and Soliman, 2017). It assists researchers in identifying potential drug candidates by simulating the interaction between the drug and its biological target. This process saves time and resources compared to traditional experimental methods.

Table 1. The basic parameters for an orally bioavailable drug (http://www.swissadme.ch/index.php).

Physiochemical properties	Predicted
Molecular Weight	≤500
Number of heavy atoms	(10-25)
Number of aromatic heavy atoms	Not specified
Fraction of C sp ³	≥0. 2
Number of rotatable bonds	≤10
Number of H-bond donor	≤5
Number of H-bond Acceptor	≤10
Molar Refractivity	(40-130)
TPSA	$(20 - 131.6 \text{ Å}^2)$
Lipophilicity	
Log P /w (iLOGP)	<5
$Log P_{/w}$ (XLOGP3)	<5
$Log P_{/w}$ (WLOGP)	<5
$Log P_{/w}$ (MLOGP)	<5
$\log P_{/w}$ (SILICOS/IT)	<5
Log K (permeation)	0 and 5



Table 2. 2D Structures and the drug-likeness of the ligands, based on the 5 scientists' rules.

S/N	Ligands			rug likeness		
		Lipinski	Ghose	Veber Yes	Egan	Muegge
ı	H ₃ C CH ₃ OH	Yes; I violation	No; 2 violations	Tes	No; I violation	No; I violatior
	3-(3-(<i>tert</i> -butylthio)-1-(4-chlorobenzyl)-5-isopropyl-1 <i>H</i> -indol-2-yl)-2,2-dimethylpropanoic acid	Yes; 0 violation	Yes	Yes	Yes	Yes
	N ³ -cyclopropyl-7-(4-isopropylbenzyl)-7 <i>H</i> -pyrrolo[3,2-f]quinazoline-1,3-diamine					
	6-chloro-7-((2-morpholinoethyl)amino)quinoline-5,8-dione	Yes; 0 violation	Yes	Yes	Yes	Yes
	F F F	Yes; 0 violation	No; I violation	Yes	No; 0 violation	No; 0 violatio
	$N-(3,5-bis(trifluoromethyl)phenyl)-5-chloro-2-hydroxybenzamide$ $CH_3 \qquad CH_3 $	No; 2 violation	No; 4 violation	No; 2 violation	No; 2 violation	No; 4 violatio
	5-methyltetrahydro-2 <i>H</i> -pyran-2-yl)butanoic acid	Yes; I violation	No; 2 violation	Yes	No; I violation	No; I violatio



S/N	Ligands	Drug likeness						
	<u> </u>	Lipinski	Ghose	Veber	Egan	Muegge		
7	HO IN OH	Yes; 0 violation	No; I violation	No; I violation	No; I violation	No; I violation		
	4-amino-1-((2R,3R,4S,5R)-3,4-dihydroxy-5-(hydroxymethyl)tetrahydrofuran-2-yl)-1,3,5-triazin-2(1H)-on							
8	HO NH N	Yes; I violation	Yes	Yes	Yes	Yes		
9	(R)-2-((6-(benzylamino)-9-isopropyl-9H-purin-2-yl)amino)butan-1-ol	Yes; 0 violation	No; I violation	Yes	No; I violation	Yes		
	4-(4-(3-(4-chloro-3-(trifluoromethyl)phenyl)ureido)phenoxy)-N-methylpicolinamide							
10	HN CH ₃	Yes; I violation	No; 3 violations	No; I violation	No; I violation	No; I violation		
	N-(3-chloro-4-((3-fluorobenzyl)oxy)phenyl)-6-(5-(((2-(methylsulfonyl)ethyl)amino)methyl)furan-2- yl)quinazolin-4-amine							
11	4-amino-1-((2R,4R,5R)-3,3-difluoro-4-hydroxy-5-(hydroxymethyl)tetrahydrofuran-2-yl)pyrimidin-2(1H)-o	Yes; 0 violation	No; I violation	Yes	Yes	Yes		
12	CH ₃	Yes;	Yes	Yes	Yes	Yes		
	H ₃ C OH NH 4-(2-(3,5-dimethyl-2-oxocyclohexyl)-2-hydroxyethyl)piperidine-2,6-dione	0 violation						



S/N	Ligands		C	rug likeness		
		Lipinski	Ghose	Veber	Egan	Muegge
3	H ₂ C CI	Yes; 0 violation	No; 2 violation	Yes	Yes	Yes
	N-(4-((3-chloro-4-fluorophenyl)amino)-7-(3-morpholinopropoxy)quinazolin-6-					
4	yl)acrylamide H ₃ CC H ₃	No;	No;	Yes	No;	No;
		2 violation	4 violation		l violation	I violation
	H ₃ CH ₃ CH ₃					
	methyl (4a%,6aR,6bS,8aR,12aX,14aS,14bR)-11-cyano-2,2,6a,6b,9,9,12a-heptamethyl-10,14-dio: 1,3,4,5,6,6a,6b,7,8,8a,9,10,12a,14,14a,14b-hexadecahydropicene-4a(2H)-carboxylate					
5	CH _h , Ch	No; 3 violation	No; 4 violation	No; 2 violation	No; 2 violation	No; 5 violation
	(S)-4-(4-((4'-chloro-4,4-dimethyl-3,4,5,6-tetrahydro-[1,1'-biphenyl]-2-yl)methyl)piperazin-1-yl) N-((4-((4-morpholino-1-(phenylthio)butan-2-yl)amino)-3-					
	N-((4-((4-morpholino-1-(phenylthio)bután-2-yl)amino)-3- ((trifluoromethyl)sulfonyl)phenyl)sulfonyl)benzamide					
6	CI CI	Yes; I violation	No; I violation	Yes	No; I violation	No; I violation
	5-(2,6-dichlorophenyl)-2-((2,4-difluorophenyl)thio)-6 <i>H</i> -pyrimido[1,6- <i>b</i>]pyridazin-6-one					
7	HN C	Yes; 0 violation	Yes; 0 violation	Yes	Yes	Yes
	H ₂ N F					
8	(S)-5-(3-fluorophenyl)-N-(piperidin-3-yl)-3-ureidothiophene-2-carboxamide	Yes; I	No; I	Yes	No;	Yes
•	CH ₃	violation	violation	1 65	I violation	1 es
	N-methyl-N-(3-(((2-((2-oxoindolin-5-yl)amino)-5-(trifluoromethyl)pyrimidin-4-yl)amino)methyl)pyridin-2-yl)methanesulfonamide					



S/N	Ligands	Drug likeness					
		Lipinski	Ghose	V eber	E gan	Muegge	
19	O CH ₃	Yes; 0 violation	Yes	Yes	Yes	Yes	
	$1-(2-methoxyethyl)-2-methyl-4, 9-dioxo-3-(pyrazin-2-ylmethyl)-4, 9-dihydro-1 \\ H-naphtho[2,3-d] imidazolar (2-methoxyethyl)-2-methyl-4, 9-dioxo-3-(pyrazin-2-ylmethyl)-4, 9-dihydro-1 \\ H-naphtho[2,3-d] imidazolar (2-methoxyethyl)-2-methyl-4, 9-dioxo-3-(pyrazin-2-ylmethyl)-4, 9-dihydro-1 \\ H-naphtho[2,3-d] imidazolar (2-methoxyethyl)-2-methyl-4, 9-dioxo-3-(pyrazin-2-ylmethyl)-4, 9-dihydro-1 \\ H-naphtho[2,3-d] imidazolar (2-methoxyethyl)-2-methyl-2-m$	-3					
20	H ₃ C H ₃	Yes; 0 violation	Yes	Yes	Yes	Yes	
21	1-((5-methoxy-2-(thiophen-2-yl)quinazolin-4-yl)amino)-3-methyl-1 <i>H</i> -pyrrole-2,5-dione	Yes; 0 violation	Yes	Yes	Yes	Yes	
	3-(4-morpholinopyrido[3',2':4,5]furo[3,2-d]pyrimidin-2-yl)phenol						
22	CH ₃	Yes; 0 violation	Yes	Yes	Yes	Yes	
	(E) - N - (7, 8 - dimethoxy - 2, 3 - dihydroimidazo [1, 2 - c] quinazolin - 5 (1H) - ylidene) nicotinal (1, 2 - c) quinazolin (1, 2 - c) quinazo	n					
23	CH ₃	No; 2 violation	No; 3 violation	Yes	Yes	No; I violation	
24	6-(2,6-dichlorophenyl)-2-((4-(2-(diethylamino)ethoxy)phenyl)amino)-8-methylpyrido[2,3-d]pyrimidin-7(8H)-one	Yes;	Yes	Yes	Yes	Yes	
	$\begin{array}{c} \\ \\ \\ \\ \\ \\ \\ \\ \\ \\ \\ \\ \\ \\ \\ \\ \\ \\ \\$	0 violation			-		



S/N	Ligands			rug likeness		
	·	Lipinski	Ghose	Veber	Egan	Muegge
25	HN CHOH	Yes; 0 violation	Yes	Yes	Yes	No; I violation
26	(55.75,8.R)-7-hydroxy-7-(hydroxymethyl)-8-methyl-5,6.7,8.13,14-hexahydro-15/H-16-oxa-4b,8a,14-triaza-5,8-methanodibenzo[b,h]cycloocta[jk/l]cyclopenta[e]-as-indacen-15-one	Yes;	Yes	Yes	Yes	Yes
		0 violation				
27	N-(cyanomethyl)-4-(2-((4-morpholinophenyl)amino)pyrimidin-4-yl)benzamide	Yes; 0 violation	No; I violation	Yes	Yes	Yes
	(E)-4*-(2-(pyrrolidin-1-yl)ethoxy)-6,12-dioxa-3-aza-2(4,2)-pyrimidina-1,4(1,3)-dibenzenacyclododecapha ene					
28	(E)-3-(4-chlorophenyl)-N-(2-((N-(2-hydroxyethyl)-4-methoxyphenyl)sulfonamido)benzyl)-N-methylacryl	Yes; I violation	No; 2 violation	No; I violation	Yes	Yes
29	8-(dibenzo[b,d]thiophen-4-yl)-2-morpholino-4H-chromen-4-one	Yes; 0 violation	Yes	Yes	Yes	No; I violation
30	CH ₃ N HO HO OH 2-(2-chlorophenyl)-5,7-dihydroxy-8-(GR,4S)-3-hydroxy-1-methylpiperidin-4-yl)-4H-chromen-4-one	Yes; 0 violation	Yes	Yes	Yes	Yes



MATERIALS AND METHODS

Materials

The materials used in this research work comprised hardware and software. The hardware is an HP computer with a processor Intel^(R) Core (TM) i5-7200U CPU @ 2.50GHz 2.71 GHz, 12GB (RAM), 1terabyte (ROM), and 64-bit by 64-based processor operating system. The software includes ChemDraw Ultra 16.0 which was used to draw the 2D structures of the compounds, Spartan 14 V 1.1.2 developed by Wavefunction Inc. was used to optimize the compounds, PyRx Virtual screening tool helps to perform the docking studies, Discovery Studio Visualizer V.17.2.0 was used to visualize the interactions of the complexes, and SwissADME (http://www.swissadme.ch/) online tools helps to predict the pharcokinetic properties of the druglikeness of the compounds.

Data Collection and Filtering

The 30 compounds used in this research work were collected from the PubChem drug databank (https://pubch em.ncbi.nlm.nih.gov). The two-dimensional structures of these compounds were obtained by inputting the SMILE ID of the compounds directly into the ChemDraw. The obtained 2D structures were imported into the Spartan 14 software one after the other to minimize the energy, employing the DFT/B3LYP approach and 6-31G* basis set (Ovaku, et al., 2020). The minimization was done to help find the best possible binding pose and affinity between the ligand and the protein target (Abdullahi, et al., 2020). The minimized compounds were then saved as 3D in Spartan file format. And subsequently saved in SD file format for the docking processes. The compounds were filtered using the online tool, SwissADME (http://www.swissadme.ch/). Some of the compounds that failed to obey three out of the five scientists' rules (Lipinski, Ghose, Veber, Egan, and Muegge) were discarded and the remaining compounds were subjected to molecular docking (Gupta, et al., 2020).

Protein and Ligands Preparations

The protein target Kras-G12D with PDB code 7ew9 used in this work was retrieved from the Protein Data Bank (PDB) (http://www.rcsb. org/) and was prepared in the Discovery Studio visualizer software, adopting the method of Umar, et.al (2023). The preparation was done by first removing the water molecules, heteroatoms, and ligands attached to the protein, after which polar hydrogen was added. The prepared protein was then saved in PDB file format. The ligand was prepared by converting them one after the other from SD file format to PDB format (Ovaku, et al., 2020). Both the ligand and protein were then imported into the PyRx virtual docking tool for the docking.

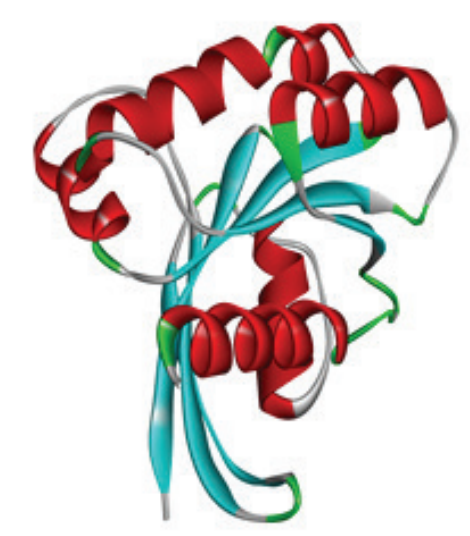


Figure 1. 3D structure of the prepared protein (KRAS-G12D).

Docking Procedure

The whole docking process was utilized with the help of the AutoDock Vina of the PyRx Virtual Screening tool and Discovery Studio Visualizer. The imported protein was saved as a macromolecule and the ligands were saved as ligands. The AutoDock Vina in the PyRx converted them into pdbqt file format when selected and a grid box with dimensions X, Y, Z (10.2115, -17.6253, 14.3348) was generated (Olaoye, *et al.*, 2024). The generated grid box helps to identify the interaction



area (binding site) of the two molecules. The molecule (ligands) was then docked into the pocket of the other molecule protein (Kras-G12D) when the grid box was forwarded. The binding energies of the complexes (Ligands-protein), were then calculated and saved in CSV file format for analysis. The ligand-protein interactions were viewed and analyzed by the Discovery Studio (Ovaku, *et al.*, 2021). Based on the binding energies calculated and the nature of interactions of the complexes, the template for the virtual design of new lead compounds was identified.

Template Identification and Design of Lead Compounds

The best-docked ligand is the ligand with the highest binding affinity and many non-bonding interactions, this was chosen as the template to structurally design new lead compounds as inhibitors of Kras-G12D (John, *et al.*, 2024). The template was imported into the online tool,

Swiss Similarity (http://www.swisssimilarity.ch/), to generate similar compounds based on their pharmacokinetics, and drug likeness features.

Drug-likeness and Pharmacokinetic properties

The pharmacokinetics properties and druglikeness behavior of the designed compounds were studied with the help of an online SwissADME tool (www.swissadme.ch/) (Mun, *et al.*, 2022). This helps to further evaluate the oral bioavailability of the compounds and point out the best design compounds.

RESULTS

This work utilized 30 already synthesized compounds that were retrieved from the PubChem drugs data bank. The results are shown mostly as figures and tables below.

Table 3. Binding energy (BE) and the number of non-bonding interactions of the complexes.

Linanda	DE/Isselment I)	Non-bonding interaction						
Ligands	BE(kcalmol-1)	H-B	π -cation	π-δ	π -anion	π-alkyl	π-S	Others
2	-8.1	2	I	I	I	2	-	I
3	-8.8	2	-	-	-	2	-	3
8	-9.0	2	-	-	-	-	I	1
11	-8.0	3	-	-	-	2	-	2
12	-9.1	-	-	-	-	3	-	2
13	-8.7	2	-	-	-	2	-	3
17	-9.0	5	I	-	-	1	-	3
*18	-10.5	6	I	-	-	1	-	3
19	-6.9	-	1	-	1	1	-	2
20	-7.5	- 1	I	-	-	2	-	2
21	-8.4	2	1	-	1	2	-	2
22	-7.9	- 1	I	- 1	-	3	-	
24	-7.8	2	I	-	-	2	-	4
26	-9.3	2	-	-	2	1	-	1
27	-9.3	-	-	- 1	-	2	-	3
29	-9.6	- 1	2	-	1	2	-	2
30	-8.2	2	1	-	-	2	-	3
Α	-7.8	6	-	-	-	-	-	3
В	-8.8	5	-	-	-	1	-	2

BE: Binding Energy; H-B: Hydrogen Bond; A: Gemcitabine; B: Irinotecan; Others: Carbon Hydrogen bond, alkyl, π - π T-shape, Halogen (Flourine) and Unfavourable acceptor-acceptor.



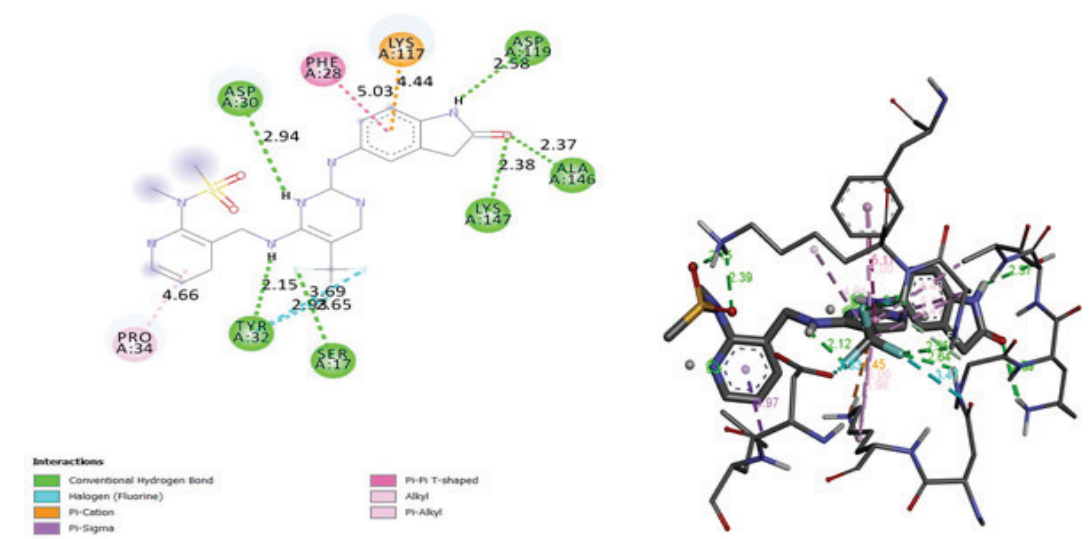


Figure 2. 2D and 3D interaction of ligand 18 and Kras-G12D.

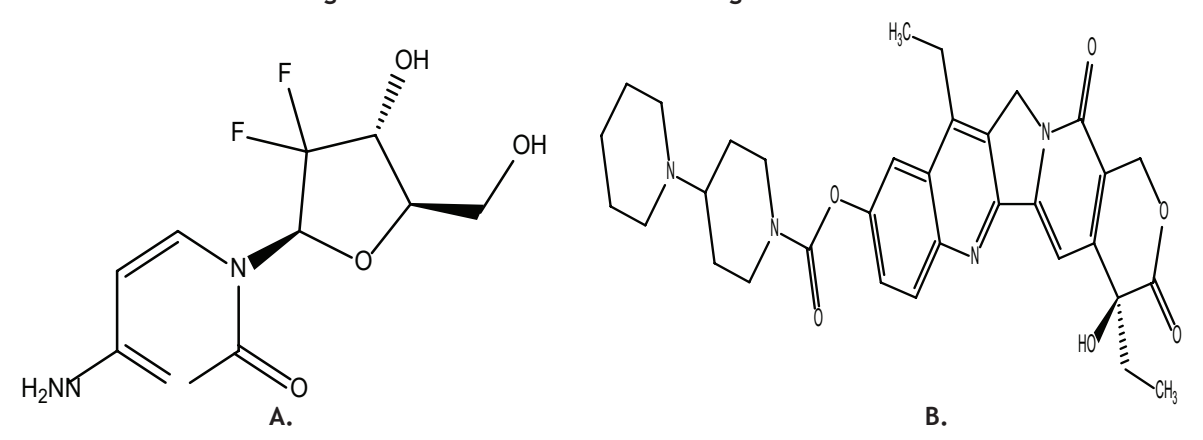


Figure 3. 2D structures of the two drugs used as reference

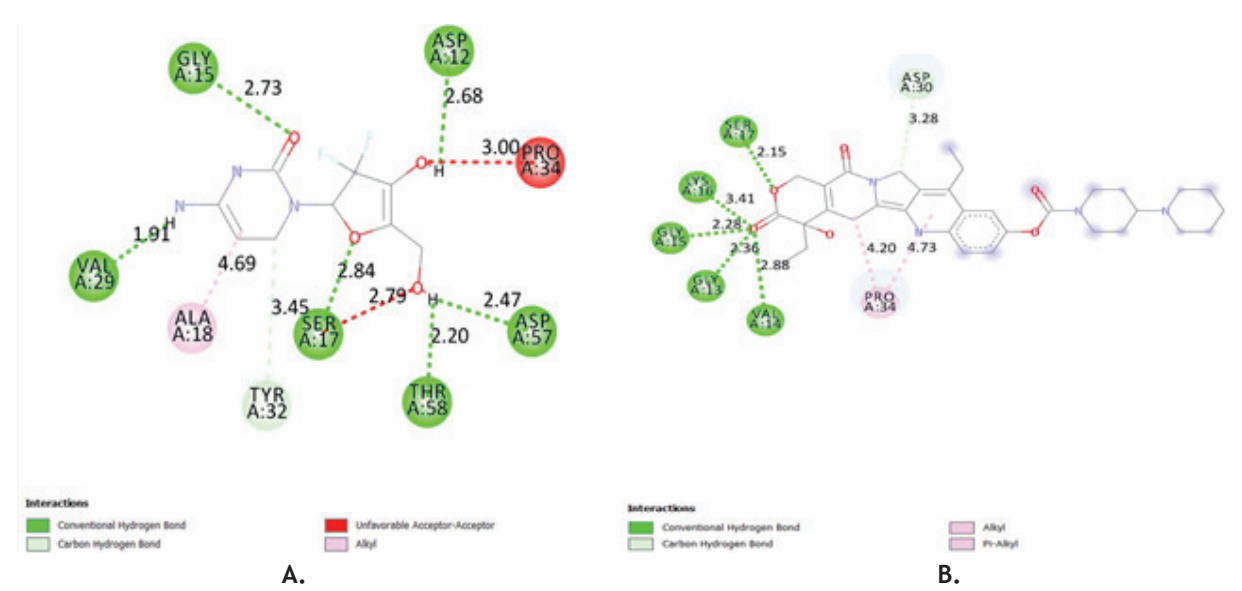
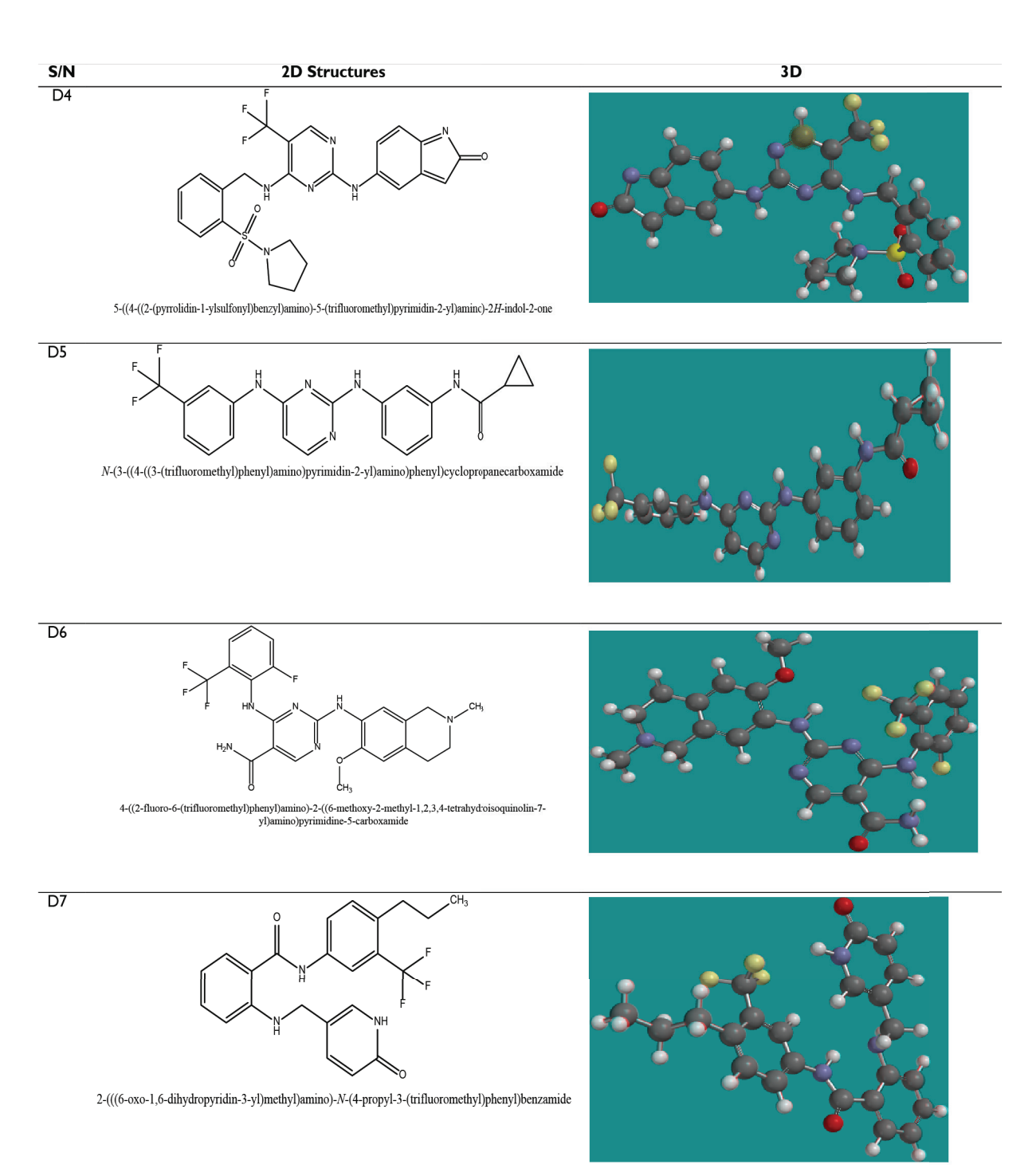


Figure 4. 2D interactions of A. Gemcitabine and B. Irritenocan with Kras-G12D.

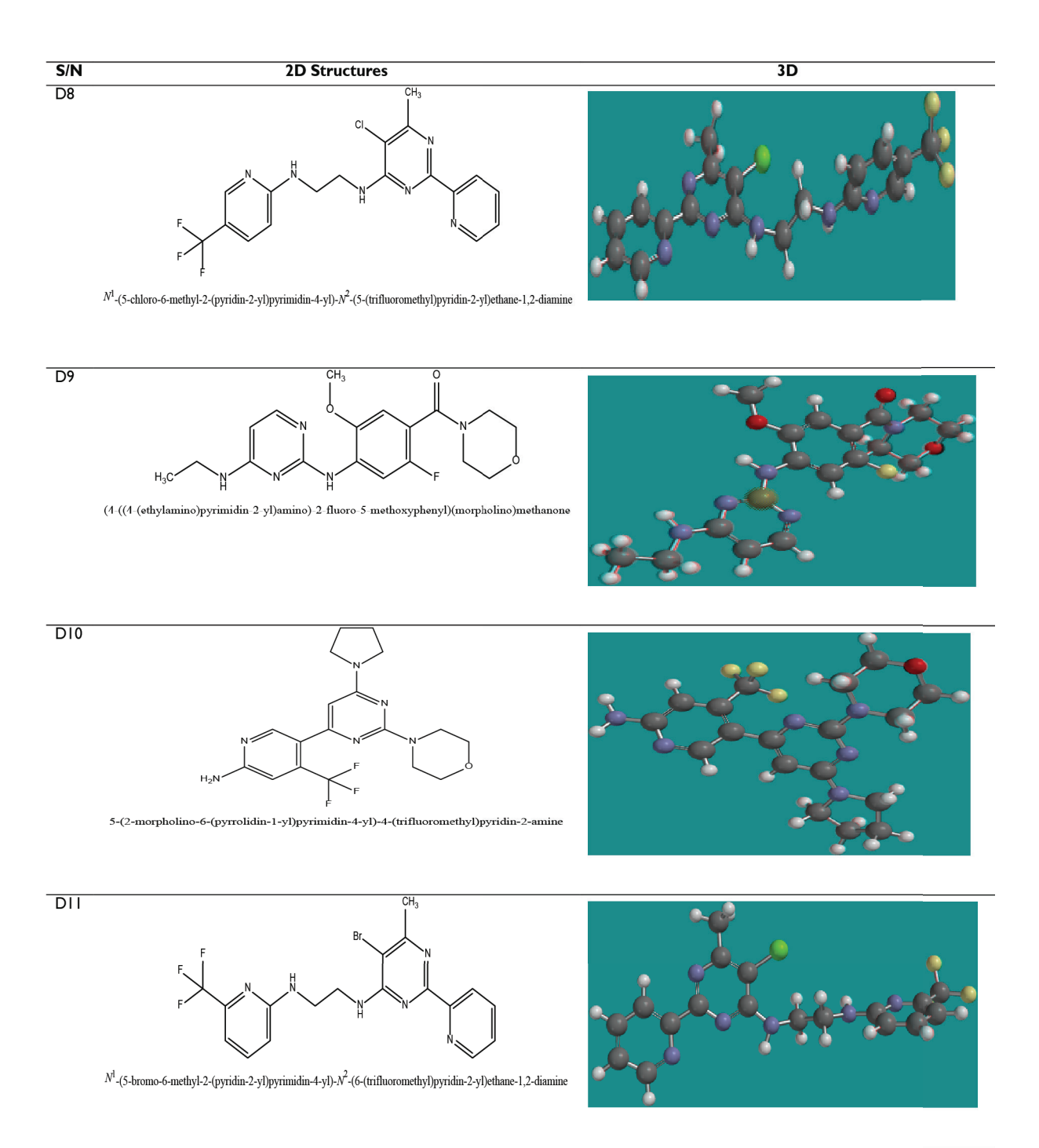


Figure 5. 2D structure of the template (ligand 18).











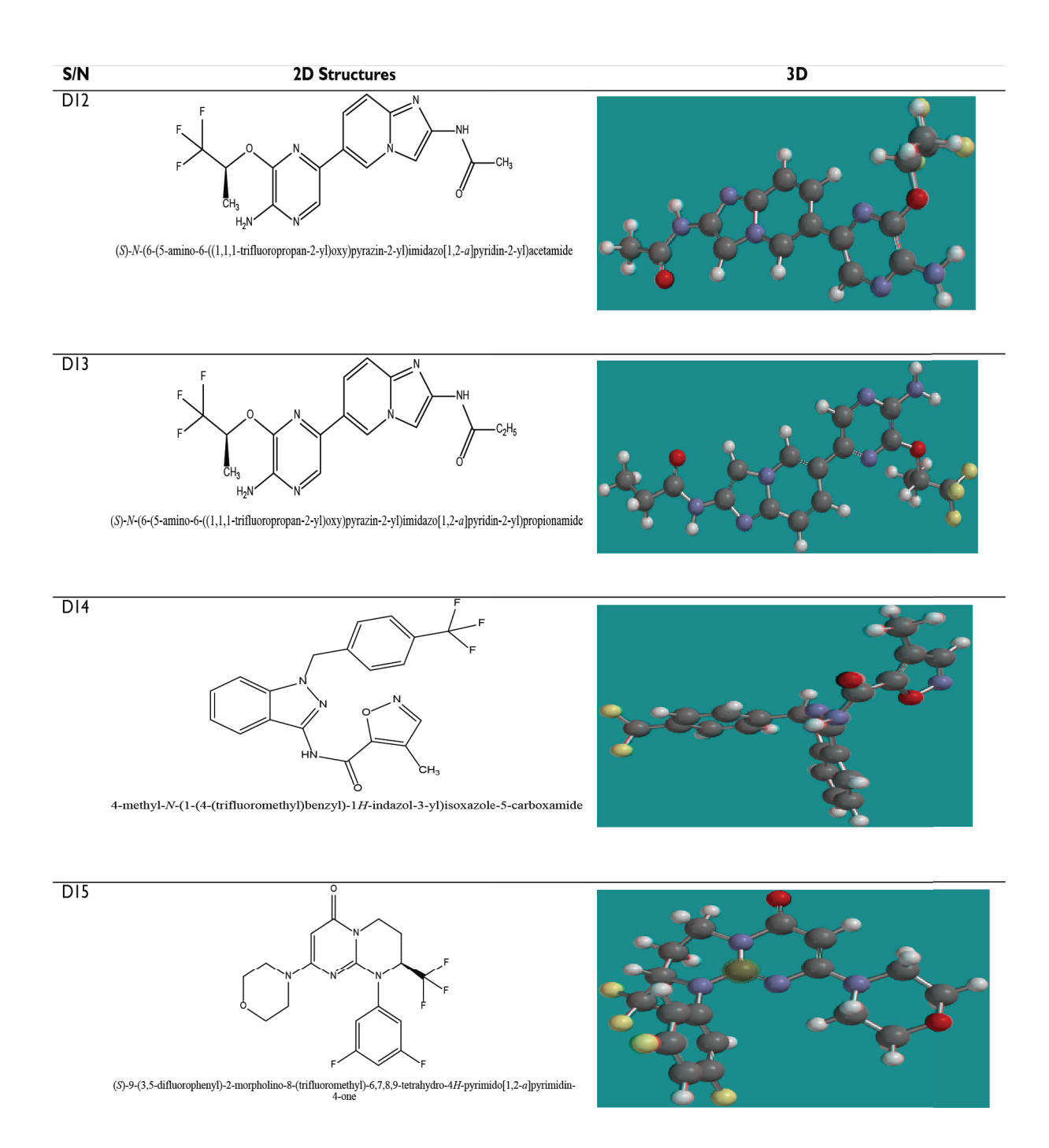




Table 5. Predicted drug-likeness parameters for the selected design compounds.

S/N	MW	H-B D	H-B A	NRB	Concessors	TPSA (Ų)	M R
	(g/mol)				Log Po/w		
DI	386.47	2	3	6	3.82	95.97	112.82
D2	335.38	2	3	4	1.86	76.43	99.52
D3	400.36	3	7	6	2.71	91.83	103.46
D4	530.52	2	10	8	3.00	125.03	136.16
D5	413.40	3	6	8	4.12	78.94	107.93
D6	490.45	3	9	7	3.83	105.40	124.91
D7	429.43	3	5	9	4.71	73.99	114.65
D8	408.81	2	7	7	3.78	75.62	100.98
D9	375.40	2	6	7	2.05	88.6 l	102.54
DI0	394.39	I	7	4	2.46	80.40	105.04
DII	453.26	2	7	7	3.86	75.62	103.67
DI2	380.32	2	8	8	2.03	107.43	91.23
DI3	394.35	2	8	7	2.38	107.43	96.04
DI4	400.35	I	7	6	3.92	72.95	99.73
D15	416.35	0	8	3	3.07	50.60	100.47

MW: Molecular weight; H-B D: Hydrogen Bond Donor; H-B A: Hydrogen bond acceptor; NRB: Number of Rotatable Bond; TPSA: Topological Polar Surface Area; MR: Molar Refractivity.

Table 6. Binding affinity and mode of interaction of the designed compounds and KRAS-G12D.

Design Comp.	BE(kcalmol-1)	Non-bonding interaction						
		Н-В	π-cation	π-δ	π-anion	π-alkyl	π-S	Others
DI	-10.2	2	-		-	2		2
D2	-8.9	4	-	-	-	I	-	3
D3	-10.1	ı	-	-	-	I	-	7
D4	-10.8	5	1	I	-	2	-	5
D5	-10.2	2	-	-	-	3	-	4
D6	-9.9	2	-	-	1	2	-	9
D7	-9.5	2	-	-	-	2	-	6
D8	-9.3	3	-	-	-	I	-	3
D9	-9.0	2	-	-	-	-	-	5
DI0	-8.3	2	1	-	-	3	-	5
DII	-9.5	3	-	-	-	1	-	5
DI2	-9.8	3	1	-	-	3	-	4
DI3	-8.3	3	-	-	2	-	ı	3
DI4	-9.8	3	-	-	-	-	ı	4
D15	-8.3	3	1	-	-	2	-	6
Gemcitabine	-7.8	6	-	-	-	-	-	3
Irinotecan	-8.8	5	-	-	-	I	-	2
Template	-10.5	6	1	-	-	I	-	3



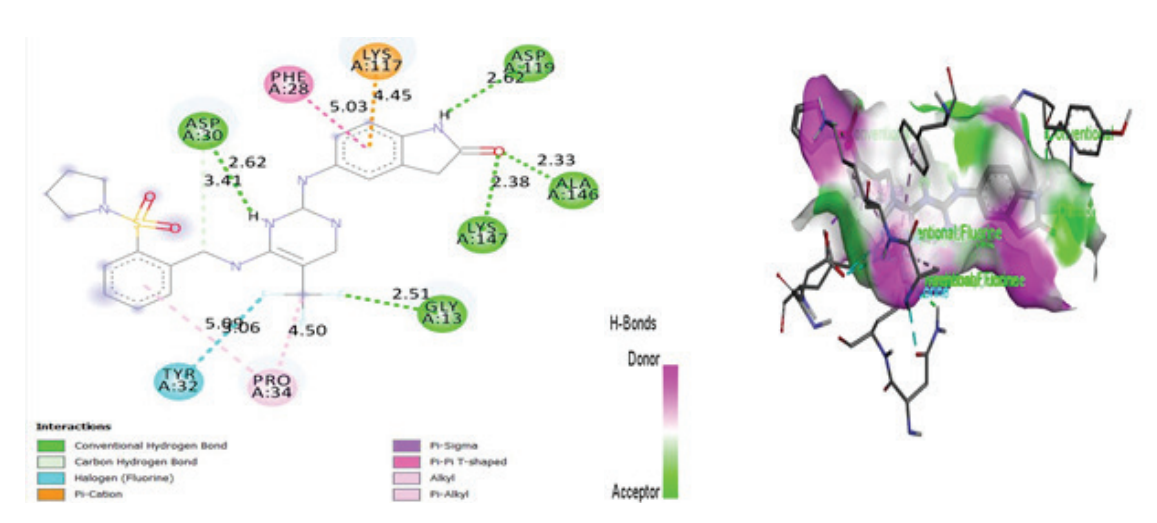


Figure 5. 2D and 3D interaction of D4 and KRAS-G12D.

DISCUSSION

Table 1 points out the predicted data used for the screening of the compounds. Out of the 30 compounds, 17 were found to be completely orally bioavailable drug candidates as shown below in Table 2. These compounds were further subjected to molecular docking studies to obtain their binding affinity and interaction modes. Figure 1 shows the 3D structure of the prepared ligand before docking. Table 3 above presents the binding affinity and the mode of interaction of the complexes. All the ligands were found to have good docking scores that range from -6.9 to -10.5 kcal mol⁻¹. From Table 3, we can see that ligand 18 with the highest binding affinity of -10.5 kcal mol⁻¹ bound strongly to the pocket of the protein target Kras-G12D than Gemcitabine and Irinotecan with B.E of -7.8 kcal mol⁻¹ and -8.8 kcal mol-1 respectively. It was however found to also have the most binding interactions with 6 hydrogen bonds, 1 pi-cation, and 2 alkyl interactions as deduced in Table 3. The conventional hydrogen bonds formed include SER17, ASP30 and ASP119, TYR32, ALA146, and LYS147 acid residues. The ASP30 was formed through the N-H bond in the pyrazine moiety with a bond distance of 2.94 Å, the SER17 and TYR32 residue was formed through

the N-H linker between the pyrazine and indoline moiety, with a bond distance of 2.15 Å and 2.95 Å respectively, ASP119 with a bond distance of 2.58 Å was formed through the N-H bond in the indoline moiety while LYS147 and ALA146 were formed through the O-O bond of the indoline moiety with a bond distance of 2.38 Å and 2.37 Å respectively. The indoline moiety also formed a pi-cation with a bond distance of 5.03 Å and a pi-pi T-shape bond of a bond distance of 4.44 Å with LYS117 and PHE28 respectively through the aromatic ring. There was also a PRO34 acid residue that formed a pi-alkyl interaction through the double bond of the N-(pyridine-2-yl) methanesulfonamide in the complex. All these interactions can be seen in Figure 2, and it indicates the stability of complex 18 as compared to the other complexes and the two drugs used in this study. The 2D and 3D interaction of the potential compound (ligand 18) with the receptor is presented in Figure 2. Figure 3 presents the 2D structures of the two drugs used as reference standard and Figure 4 displays their binding interaction with the protein target. This was however compared with the most potential compound in our dataset (ligand 18). Gemcitabine was found to have 6 conventional hydrogen bonds, 1 alkyl, 1 carbon-hydrogen bond, and 1 unfavorable acceptor-acceptor interaction,



while Irinotecan on the other hand was found to have only 4 conventional hydrogen bonds, 1 alkyl, and 1 pi-alkyl interactions. Based on these results, ligand 18 shows a better drug candidacy than the commercially sold anti-cancer drugs.

To develop a more potent anti-pancreatic cancer drug from our dataset, ligand 18, which has proven to be the most promising druglike compound was used to design several new compounds. Figure 5, displays the 2D structure of ligand 18 used to perform the structure base design through structure adjustment and reform in the **SwissSimilarity** (http://www.swisssimilarity.ch/) of the SwissDrugDesign (https://www.expasy.org/ resources/swissdrugdesign) online tool (Sucharitha, et al., 2022). The SMILE ID of the template was imported into the tool, a synthesizable class of compounds was selected, and a library of screened compounds (InnovaPharm Tang) was generated, utilizing the pharmacophore method (Zoete, et al., 2016).

For simplicity, only 15 out of the many generated compounds were selected based on their drug-likeness properties when evaluated in the SwissADME tool. Table 5, shows the 2D and 3D structure of all 15 compounds with their IUPAC name while Table 6 shows the drug-likeness properties of the designed compounds. All the designed compounds have good binding energies that range from -8.3 to -10.8 kcal mol⁻¹, and noncovalent bonds of interaction as displayed in Table 6. Compounds D1, D3, D4, and D5 are however good potential designed compounds as compared to the commercially sold pancreatic cancer drugs, Gemcitabine and Irinotecan. Nevertheless, our main discussion will be focused on D4, which is the best-designed compound. It displays good physiochemical and pharmacokinetic properties. Compound D4 passed all the five scientific rules of good oral drug bioavailability test. Even though it violates 1 of the Lipinski's rules of five (MW>500). Generally, Lipinski's rule states that an orally active drug has no more than one violation of the following

criteria, "no more than 5 hydrogen bond donors, no more than 10 hydrogen bond acceptors, a molecular weight of less than 500 g mol-1, and a calculated octanol-water partition coefficient of less than 5" (Lohit, et al., 2024). Compound D4 has the highest BE of -10.8 kcal mol⁻¹, and the pictorial interaction of the complex has been displayed in Figure 6. It was found to have 5 hydrogen bond interactions, 2 pi-alkyl, 1 pi-cation, 1 halogen (Fluorine), 1 pi-sigma, 1 Carbon-hydrogen bond, and 1 pi-pi T-shaped bond. The hydrogen bond formed 2 acid residues, LYS147 and ALA146 through the O-O bond, and 1 ASP119 acid residue through the N-H of the indoline moiety. It also forms 1 ASP30 and 1 GLY13 residue through N-H and F in the pyridine and 5-trifluoro (pyridine) moiety respectively. Several other hydrophobic interactions were also formed, and all these non-covalent bonds contribute to the high binding affinity associated with D4.

CONCLUSION

In the course of designing a new and more potent drug candidacy against KRAS-G12D in pancreatic cancer, 30 compounds retrieved from the PubChem drug data bank were subjected to a structured virtual screening. A lead-hit compound (ligand 18) against KRAS-G12D was identified and was successfully used to design even better candidate drugs. The result of our work shows that the template, the best four designed compounds are good oral drug bioavailability compounds than the existing drugs. This work provides insight into the discovery of new cancer drugs. Conclusively, these compounds should be the starting material for the synthesis of new anti-pancreatic cancer.

ACKNOWLEDGMENTS

The corresponding author acknowledged the scholarly advice and encouragement of Muhammad Tukur Ibrahim of ABU Zaria and Mustapha Abdullahi of KASU.



REFERENCES

- Abdullahi, M., Uzairu, A., Shallangwa, G.A., Arthur, D.E., Umar, B.A., and Ibrahim, M.T., 2020, Virtual molecular docking study of some novel carboxamide series as new antitubercular agents, *European Journal of Chemistry*, 11(1), 30-36.
- Banegas-Luna, A.J., Cerón-Carrasco, J.P., and Pérez-Sánchez, H., 2018, A review of ligand-based virtual screening web tools and screening algorithms in large molecular databases in the age of big data, *Future medicinal chemistry*, **10**(22), 2641-2658.
- Bray, F., Ferlay, J., Soerjomataram, I., Siegel, R.L., Torre, L.A., and Jemal, A., 2018, Global cancer statistics 2018: GLOBOCAN estimates of incidence and mortality worldwide for 36 cancers in 185 countries, *CA*: a cancer journal for clinicians, 68(6), 394-424.
- Broomhead, N.K., and Soliman, M.E., 2017, Can we rely on computational predictions to correctly identify ligand binding sites on novel protein drug targets? Assessment of binding site prediction methods and a protocol for validation of predicted binding sites, *Cell biochemistry and biophysics*, **75**, 15-23.
- Carioli, G., Malvezzi, M., Bertuccio, P., Boffetta, P., Levi, F., La Vecchia, C., and Negri, E., 2021, European cancer mortality predictions for the year 2021 with focus on pancreatic and female lung cancer, *Annals of Oncology*, **32**(4), 478-487.
- da Silva Rocha, S.F., Olanda, C.G., Fokoue, H.H., and Sant'Anna, C.M., 2019, Virtual screening techniques in drug discovery: review and recent applications, *Current topics in medicinal chemistry*, **19**(19), 1751-1767.
- Dai, M., Chen, S., Teng, X., Chen, K., and Cheng, W., 2022, KRAS as a key oncogene in the clinical precision diagnosis and treatment of pancreatic cancer, *Journal of Cancer*, **13**(11), 3209.
- Ducreux, M., Cuhna, A.S., Caramella, C.,

- Hollebecque, A., Burtin, P., Goéré, D., *et al.*, 2015, Cancer of the pancreas: ESMO Clinical Practice Guidelines for diagnosis, treatment and follow-up, *Annals of oncology*, **26**, v56-v68.
- Gupta, P.P., Bastikar, V.A., Bastikar, A., Chhajed, S.S., and Pathade, P.A., 2020, Computational screening techniques for Lead design and development, *Computer-aided drug design*, 187-222.
- Gupta, V., Bankar, N., and Chandankhede, M., 2021, The COVID-19-An Agent for Bioterrorism?, Journal of Pharmaceutical Research International, 33(40B), 279-284.
- Hofmann, M.H., Gerlach, D., Misale, S., Petronczki, M., and Kraut, N., 2022, Expanding the reach of precision oncology by drugging all KRAS mutants, *Cancer Discovery*, **12**(4), 924-937.
- http://www.rcsb.org/pdb/home/home.do
- John, A., Uzairu, A. Shallangwa, G.A., and Uba, S., 2024, Theoretical Investigation and Design of Bioactive Quinoline Derivatives as Inhibitors of DNA Gyrase of Salmonella Typhi, *Malaysian Journal of Pharmaceutical Sciences*, **22**. 1-20.
- Lohit, N., Singh, A.K., Kumar, A., Singh, H., Yadav, J.P., Singh, K., and Kumar, P., 2024, Description and *In silico* ADME Studies of US-FDA Approved Drugs or Drugs under Clinical Trial which Violate the Lipinski's Rule of 5, *Letters in Drug Design & Discovery*, 21(8), 1334-1358.
- Mun, C.S., Hui, L.Y., Sing, L.C., Karunakaran, R., and Ravichandran, V., 2022, Multi-targeted molecular docking, pharmacokinetics, and drug-likeness evaluation of coumarin-based compounds targeting proteins involved in development of COVID-19, Saudi journal of biological sciences, 29(12), 103458.
- Olaoye, I., Akhigbe, G., Awotula, A., Oso, B., Agboola, O., Adebayo, A., and Banwo, R., 2024, Molecular Insights on Binding Interactions of Cyclooxygenase and Lipoxygenase Activities on Malondialdehyde in Naphthalene-Exposed Wistar Rats, *Sciendo Acta Medica Bulgarica*, 51(s2), 120-142.



- Ovaku, I.M., Adeniji, S.E., Habib, K., and Adeiza, A.A., 2021, Molecular docking of some novel quinoline derivatives as potent inhibitors of human breast cancer cell line, *Lab-in-Silico*, 2(1), 30-37.
- Ovaku, M.I., Abech, S.E., Shallangwa, G.A., and Uzairu, A., 2020, *In Silico* Elucidation of Some Quinoline Derivatives with Potent Anti-Breast Cancer Activities, *The Journal of Engineering and Exact Sciences*, **6**(1), 0008-0014.
- Ovaku, M.I., Abechi, S.E., Shallangwa, G.A., and Uzairu, A., 2020, QSAR and Molecular Docking Studies of novel thiophene, pyrimidine, coumarin, pyrazole, and pyridine derivatives as Potential Anti-Breast Cancer Agent, *Turkish Computational and Theoretical Chemistry*, 4(1), 12-23.
- Patel, A.R., Patel, H.B., Mody, S.K., Singh, R.D., Sarvaiya, V.N., Vaghela, S.H., and Tukra, S., 2021, Virtual screening in drug discovery, Journal of Veterinary Pharmacology and Toxicology, 20(2), 1-9.

- Sardar, H., 2023, Drug-like potential of Daidzein using SwissADME prediction: *In silico* Approaches, *PHYTONutrients*, 02-08.
- Sucharitha, P., Reddy, K.R., Satyanarayana, S.V., and Garg, T., 2022, Absorption, distribution, metabolism, excretion, and toxicity assessment of drugs using computational tools. in Computational approaches for novel therapeutic and diagnostic designing to mitigate SARS-CoV-2 infection, pp. 335-355, Academic Press.
- Umar, A.B., Uzairu, A., Ibrahim, M.T., Usman, A., Habib, A., and Usman, B., 2023, Investigation of Novel Imidazole Analogues with Terminal Sulphonamides as Potential V600E-BRAF Inhibitors Through Computational Approaches, *Chemistry Africa*, 6(6), 3027-3038.
- Zoete, V., Daina, A., Bovigny, C., and Michielin, O., 2016, SwissSimilarity: A Web Tool for Low to Ultra High Throughput Ligand-Based Virtual Screening., *J. Chem. Inf. Model.*, **56**(8), 1399-1404.